Phys. Status Solidi A **210,** No. 1, 175–180 (2013) / **DOI** 10.1002/pssa.201200567

physica status solidi a
www.pss-a.com
applications and materials science

The role of extended defects in device degradation

Sokrates T. Pantelides[*,1,2]

[1] Departments of Physics and Astronomy and of Electrical Engineering and Computer Science, Vanderbilt University, Nashville, TN 37235, USA
[2] Materials Science and Technology Division, Oak Ridge National Laboratory, Oak Ridge, TN 37831, USA

Received 8 August 2012, accepted 9 October 2012
Published online 7 December 2012

Keywords degradation, grain boundaries, interfaces, impurities

[*] e-mail pantelides@vanderbilt.edu, Phone: +1 615 343 4321, Fax: +1 615 343 6589

Grain boundaries and dislocations are well known to cause trouble in electronic devices, but in most cases they can be avoided by using single crystal films and eliminating or suppressing dislocation densities. Hetero-interfaces, on the other hand, are essential features of devices. This papers reviews several topics from the author's published work, combining theoretical calculations with experimental data (microscopy, electrical measurements) to illustrate the interplay of impurities with extended defects, especially interfaces: dopant segregation in grain boundaries of polycrystalline Si, the role of hydrogen in the degradation of the Si–SiO_2 interface in Si-based metal-oxide-semiconductor field-effect transistors (MOSFETs), the role of carbon, nitrogen, and hydrogen in the quality and degradation of the SiC–SiO_2 interface in SiC-based MOSFETs, and the role of vacancies in room-temperature degradation of III–V high-mobility electron transistors by the formation of microvoids.

1 Introduction With the advent of high-performance computers, quantum mechanical calculations in solids have become a very powerful tool to probe properties and, in combination with experimental data, determine the atomic-scale processes that underlie observed phenomena. Modern technology amounts to fabricating structures and controlling defects in a way that takes advantage of their beneficial properties (e.g. doping of semiconductors) while avoiding defects that have a negative effect at the outset or gradually lead to degradation.

Extended defects such as grain boundaries and dislocations generally have a negative effect, e.g. they act as centers for carrier recombination, and are avoided. Most electronic devices are made of single-crystal films in which dislocation densities are suppressed to acceptable levels. For example, Si devices are fabricated using single crystals with no dislocations. Until recently, heavily doped polycrystalline Si was used as gate "metal" in Si MOSFETs. In III–V devices, suppressing dislocations is more difficult but achievable. Hetero-interfaces, on the other hand, which can be viewed as planar defects like grain boundaries, are an essential element of devices. In Si MOSFETs, the Si–SiO_2 interface is a key element that controls carrier mobility in the channel and the region where device degradation often originates. In contrast, the inability to fabricate high quality interfaces between a III–V semiconductor and a dielectric is the reason that III–V-based MOSFETs are not available. High-mobility electron transistors (HEMTs) are the preferred structures instead. SiC is a special case whose native oxide is the same as that of Si, namely SiO_2. Fabricating high-quality SiC–SiO_2 interfaces, however, has been a challenge.

In this paper, we will give a brief review of a few extended defects and their role in device degradation, with emphasis on the interaction of impurities with interfaces. We start with an example of impurity segregation in grain boundaries and then review the role of hydrogen in causing degradation at the Si–SiO_2 interface. We then contrast the Si–SiO_2 and SiC–SiO_2 interfaces and identify the origin of problems in the latter. We close with a brief discussion of a case in III–V-based HEMTs where interface degradation by the formation of microvoids is caused by room-temperature diffusion mediated by vacancies. Based on a plenary talk at EDS-2012, the paper will not attempt any broader coverage of the field beyond the author's work.

2 Methods Theoretical calculations for the various investigations were performed using density functional

theory, the method of choice for quantum-mechanical calculations for solids. Pseudopotentials are used to mimic the effect of the atomic cores. Supercells with periodic boundary conditions are used to enable the use of plane waves as a basis set. The local density approximation with generalized gradient corrections is used for exchange and correlation.

The research described here has been collaborative with experimental groups over many years: Atomically-resolved scanning transmission electron microscopy [Z-contrast images and electron-energy-loss spectroscopy (EELS)] by S. J. Pennycook and his group at Oak Ridge National Laboratory, electrical measurements by R. D. Schrimpf and D. M. Fleetwood at Vanderbilt University and SiC oxidatiton and electrical measurements by L. C. Feldman (Vanderbilt) and J. R. Williams (Auburn University) and their groups.

3 Impurity segregation in grain boundaries

Heavily doped polycrystalline Si has been used as the gate "metal" in microelectronics. It has been known that dopant impurities, typically As, segregate in grain boundaries where they are inactive. Engineers would like to know whether the phenomenon is intrinsic or it is caused by defect structures in the grain boundaries that in principle can be avoided. Calculations that were available at the time found minimal energy gain if a substitutional As atom is moved from the bulk crystal to the grain boundary, suggesting that defect structures within the grain boundary are responsible.

While experimental work was being pursued to obtain Z-contrast images of an As-doped Si bicrystal, theoretical calculations led us to predict that As impurities would segregate in *selected* columns of a pristine Si grain boundary in the form of dimers [1]. Energy gain comes from the two As atoms pushing away from each other and achieving threefold coordination, which is their normal preference as in AsH_3 (three bonds are formed while the remaining two As valence electrons occupy a non-bonding p state as a "lone pair"). In the bulk crystal, such a relaxation entails significant elastic-energy cost (As pairs can form in bulk Si by binding to a vacancy [2]). The key is that in select columns of a grain boundary, the elastic-energy cost is small and the relaxation wins. It is intriguing that the As dimer binding energy arises from mutual repulsion! The net conclusion is that As segregation in Si grain boundaries is an intrinsic phenomenon and does not require defective grain boundary structures.

Arsenic impurities were subsequently imaged in select columns (Fig. 1) [3]. This was the first ever direct imaging of segregated impurities in a grain boundary. Without the theory, imaging would not reveal whether defect structures are involved, the origin of energy gain, or the cause for column selectivity. Theory also predicted that, in some grain boundaries, As segregation may reverse the energy ordering of different reconstruction modes, suggesting that *impurity-induced grain boundary structural transformations* may be possible in poly-Si.

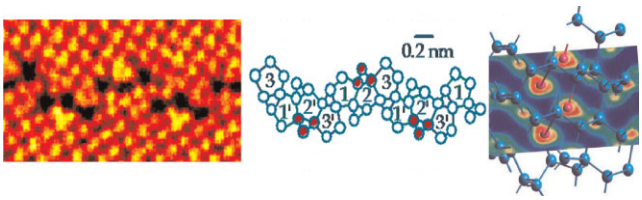

Figure 1 (online color at: www.pss-a.com) Left: Z-contrast image of a Si grain boundary. Bright columns contain As impurities as illustrated in the schematic diagram in the middle panel. Right: calculated electron density. From Refs. [1, 3].

Such a phenomenon was in fact observed soon afterwards in a different material, MgO, and confirmed by theory [4]. Z-contrast images of an MgO grain boundary revealed a structure that was very different from the accepted structure (Fig. 2). It was noted that some columns were brighter than others. EELS was used to establish that the bright columns contained Ca (Fig. 2). Theory then took over and showed that the accepted grain boundary structure is indeed the ground state, but, when Ca impurities are inserted, the new structure has lower energy. Thus, the combination of Z-contrast images, EELS, and theory demonstrated a case of impurity-induced structural transformation.

4 Degradation at the Si–SiO_2 interface

Oxidation of Si leads to very abrupt, "perfect" interfaces that are at the heart of modern microelectronics. The primary interfacial point defects are "dangling bonds", i.e. Si atoms with only three neighbors. Hydrogen is intentionally introduced in MOSFETs to passivate dangling bonds, which results in higher carrier mobilities in the channel. A schematic diagram of the interface density of defect states after passivation is shown in Fig. 3. The small bump in the middle is due to still unpassivated dangling bonds and the rise near the band edges is due to "suboxide bonds", i.e. Si–Si bonds on the oxide side of the interface that tend to be somewhat longer than normal Si–Si bonds (they can also be thought of as O vacancies), giving bonding and antibonding states near the band edges. Otherwise, the Si–SiO_2 interface is quite perfect [5], except for occasional steps.

Over the years, many undesirable phenomena, observed in MOSFETs under different conditions and causing varying degrees of degradation, have gradually been attributed

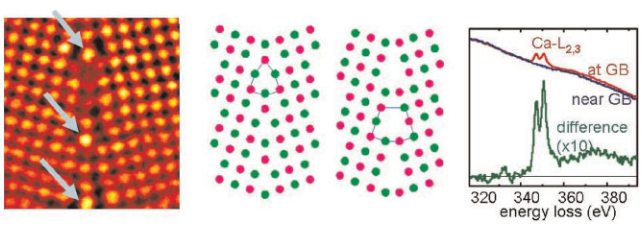

Figure 2 (online color at: www.pss-a.com) Z-contrast image of a MgO grain boundary, atomic-scale structure derived from the image, accepted structure, and EELS spectra at and near the grain boundary. From Ref. [4].

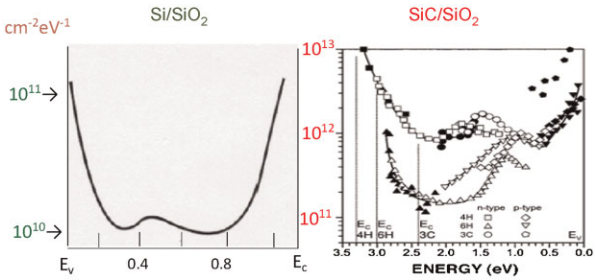

Figure 3 (online color at: www.pss-a.com) Interface density of defect states at the Si–SiO_2 interface after passivation (left) and at the SiC–SiO_2 interface after attempted passivation with H (right, Ref. [6]).

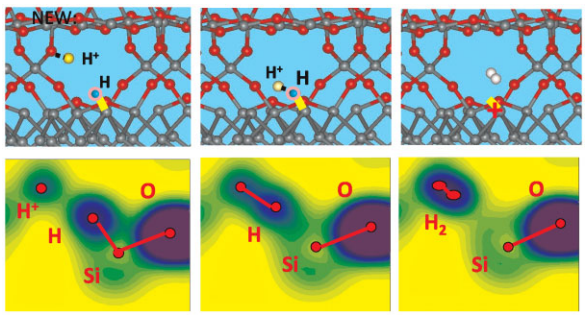

Figure 4 (online color at: www.pss-a.com) Top: schematic diagram illustrating the depassivation of a dangling bond by H^+. Bottom: Electron density at the corresponding steps. From Ref. [9].

directly or indirectly to hydrogen causing depassivation of dangling bonds at the Si–SiO_2 interface. In a multiyear collaboration by the author with engineers R. D. Schrimpf and D. M. Fleetwood (Vanderbilt) along with students and post-docs, we pursued extensive first-principles calculations of hydrogen configurations and interfacial reactions in MOSFETs in the context of pertinent experimental data, both old and new [7, 8]. Here is a summary of key results.

Under radiation conditions (X-rays), electron-hole pairs are generated in the gate oxide of a MOSFET. Under positive bias, electrons are swept out through the gate and holes head more slowly toward the interface, occasionally getting trapped inside the oxide at O vacancies and other defects. It has long been recognized that holes release H^+ within the oxide and that, under positive bias, H^+ also heads for the interface where it can depassivate dangling bonds by forming H_2 molecules. The details of these reactions, however, were the subject of much debate. Through quantum mechanical calculations, the following detailed descriptions of the pertinent atomic-scale processes were obtained.

Hydrogen is directly released as H^+ at most defects where it is initially bound. If it were released as neutral H, the electron would be at an energy level quite high in the SiO_2 energy gap. The presence of holes, therefore, leads to electron–hole recombination during H release with a substantial gain in energy.

H^+ migrates to the interface with an activation barrier that varies in the range 0.4–0.8 eV in the amorphous oxide. Once it arrives at the interface, it can migrate in the interfacial plane with a small activation energy, only ~0.3 eV, whereas the barrier to cross the interface is larger, ~0.8 eV. It can then easily find suboxide bonds where it can occupy the bond center and create a positively charged defect. Once trapped there, the barrier to get out into the oxide is ~1 eV while the barrier to get out into the Si substrate is ~1.5 eV. In the interfacial plane, H^+ can also find passivated dangling bonds, interact directly with the bonded H, form H_2, which migrates away, and leave behind positively charged dangling bonds (Fig. 4) [9]. That is the main cause of X-ray radiation-induced degradation.

Degradation phenomena are usually studied experimentally by going to high doses or high temperatures for speedier results, followed by modeling that extrapolates to operating conditions. In the case of X-ray degradation, an unusual phenomenon was observed, known as enhanced low-dose-rate sensitivity (ELDRS; Fig. 5) [10, 11]. At low dose rates, degradation is enhanced. Theoretical calculations provided an elegant explanation of the puzzle [12]. At low dose rates, a relatively low density of holes is generated and releases H^+. Both holes and H^+ head for the interface and sufficient H^+ arrive at the interface to cause degradation. At high dose rates, much higher hole densities are generated. The holes get to the interface faster than whatever H^+ they release and get trapped at near-interface vacancies and interfacial suboxide bonds. These newly created positively-charged defects create an electrostatic fence and shield the interface from the H^+ onslaught. Hence, the reduced degradation.

Yet another radiation-induced phenomenon is the deactivation of dopants in the Si substrate [13]. It was recognized that H^+ crossing the interface is again the culprit. Again the details of the underlying reactions were not clear. The topic of dopant deactivation by hydrogen received extensive attention by both theory and experiments in the 1980s [14–19], but modeling of the radiation-induced data was still not definitive. More recent calculations reproduced the data, providing quantitative explanation of the behavior in the three different regions of irradiation bias (Fig. 5) [20]. Under accumulation conditions, the bias is negative and H^+ in the oxide heads toward the gate. Under positive bias,

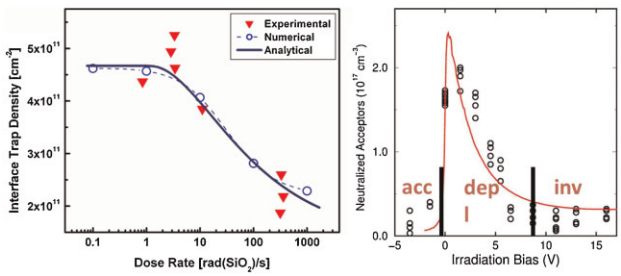

Figure 5 (online color at: www.pss-a.com) Left: ELDRS data and theory. Right: Boron acceptor depassivation, data and theory (red curve). Accumulation, depletion and inversion regions are indicated. From Ref. [12]. Right: Radiation-induced deactivation of boron dopants. From Ref. [13].

initially there is a depletion region near the interface where holes are absent so that H^+ freely moves into the substrate and deactivates the boron dopants. At larger positive bias, inversion occurs; electrons are present near the interface and convert the arriving H^+ to neutral so that its migration into the substrate relies strictly on diffusion, which is relatively slow at room temperature.

A final example of interface degradation by hydrogen that does not involve radiation is the phenomenon known as negative bias temperature instability (NBTI) [21, 22]. Under negative bias and moderate temperatures, the interface defect density increases. Once more, the cause was traced to the depassivation of dangling bonds. The general consensus is that the NBTI conditions, i.e. the presence of holes near the interface and the moderate temperature cause the spontaneous release of the hydrogen [22].

Calculations, however, led us to different conclusions [23]. It was found that the activation barrier for spontaneous H release is too high, of order 1.9 eV in the absence of holes and ~1.6 eV in the presence of holes. The electric field may lower the barrier by another 0.1 eV. The resulting activation barrier is too large for a room-temperature effect. An alternative explanation was proposed: hydrogen mediated release by the formation of H_2 molecules. This time the hydrogen needs to come from the substrate because the bias is negative. Hydrogen is present in the substrate because during the final anneal to passivate interfacial dangling bonds, some hydrogen crosses into the substrate and deactivates a fraction of the dopants that is tolerable. A calculation of the effective activation energy for the hydrogen-mediated release based on a quasi-equilibrium theory by Jeppson and Svensson [21] gave a value of 0.36 eV, in line with observations.

5 The SiC–SiO_2 interface Silicon electronics does not work very well in high-temperature or high-power environments because of the relatively small energy gap of Si. The search for a wide-gap semiconductor with good heat conduction properties has been going on for some time. III–V compounds have well-known problems with the lack of a suitable dielectric to make MOSFETs. Silicon carbide is unique because it has a good band gap, good thermal conductivity, and its native oxide is none other but SiO_2. When SiC–SiO_2 interfaces were first fabricated more than 15 years ago, the carrier mobility in the SiC substrate near-interface region was found to degrade from its bulk value of around 800 $cm^2 V^{-1} s^{-1}$ to an unacceptably low value of order 1 $cm^2 V^{-1} s^{-1}$ (in contrast, at the Si–SiO_2 interface, the interfacial mobility is typically reduced only by a factor 2). Measured densities of interface defect states at the SiC–SiO_2 interface were found to be very large by comparison with the Si–SiO_2 interface (Fig. 3). The defects were attributed to residual carbon at the interface. Attempts to passivate these defects using hydrogen failed [6].

In a multiyear collaboration by the author doing theory, L. C. Feldman (Vanderbilt University) and J. R. Williams (Auburn University) doing oxidation and electrical measurements, with microscopy by G. Duscher and S. J. Pennycook, along with students and post-docs, several advances were made [24]. The first key result was an attempt to passivate with nitrogen, which worked [25]. Post-oxidation anneal in NO reduces the interface defect density substantially (Fig. 6) and carrier mobility climbs to around 50 $cm^2 V^{-1} s^{-1}$, high enough to yield viable commercial devices. More recently, additional passivation by hydrogen was also found to occur (Fig. 6) if monatomic H is used [26]. More specifically, H_2 was passed through a Pt layer where it gets cracked.

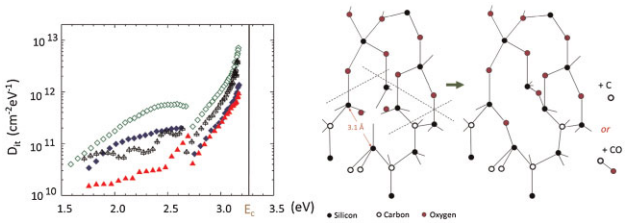

Figure 6 (online color at: www.pss-a.com) Left: Latest experimental results on interface defect density at the SiC–SiO_2 interface: green – as oxidized; blue – NO only; black – H only; red – NO followed by H. From Refs. [24, 26]. Right: Schematic diagram showing the elemental step of SiC oxidation. From Ref. [24].

On the theoretical side, the basic oxidation mechanism was identified (Fig. 6). Oxygen atoms arriving at the interface kick C atoms out and replace them to form Si–O–Si bridges, opening the ring structure. C atoms can capture an arriving O and form CO, which then exits through the growing oxide (C clusters can form inside the oxide but they are eliminated by a post-oxidation anneal in oxygen [27]). C atoms can also enter the SiC substrate.

Residual carbon at the interface can form individual defects, but more likely, the preponderance of evidence led to the conclusion that a Si–C–O bonded interlayer is present [24, 26]. After NO anneal, nitrogen is also incorporated, resulting in a Si–C–O–N interlayer. Finally, with H added, the net result is a Si–C–O–N–H bonded interlayer. Evidence for such an interlayer has been provided by Z-contrast imaging and EELS (Fig. 7).

Carbon entering the SiC substrate was identified as an endemic cause of mobility degradation [28]. As interstitials,

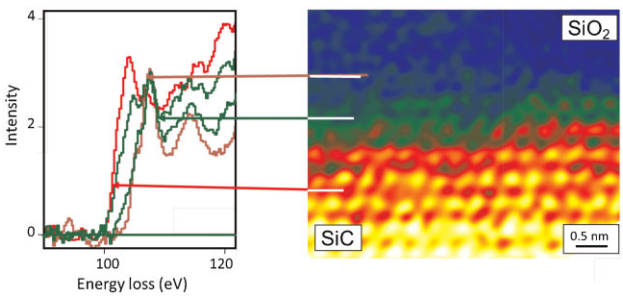

Figure 7 (online color at: www.pss-a.com) Left: EELS spectra at the SiC–SiO_2 interface. Right: Z-contrast image of a SiC–SiO_2 interface showing an interlayer as described in the text. From Ref. [26].

carbon atoms are quite mobile and can form interstitial pairs. These pairs are not mobile but are negatively charged in the commonly used n-type SiC, causing Coulomb scattering. The identification of the C di-interstitial was corroborated by systematic interpretation of several experimental measurements.

Finally, there are several other reasons that the SiC–SiO_2 interface is rougher than the Si–SiO_2 interface. Calculations [29] demonstrated that it is just more difficult to form a well-bonded interface on SiC largely because of the nature of the atomic arrangements and the smaller bond lengths. Furthermore, in the case of the Si–SiO_2 interface, calculations have demonstrated that the oxide grows in a way that is similar to epitaxial growth of thin films [5]. As O atoms are "deposited" at the advancing interface, they enter into Si–O–Si protrusions. Interfacial diffusion then helps smooth out the interface. But a critical step, the one that actually needs the relatively high temperature of over 800 °C because of a high activation barrier, is the "desorption and re-absorption" of O. In this case, O atom "desorb" and enter the Si substrate where they migrate easily [30] and can even cluster [31], but they often -get "reabsorbed at the interface. This kind of smoothing is not possible in the case of the SiC–SiO_2 interface because O cannot easily enter the substrate (the solubility of O in SiC is three orders of magnitude smaller than in Si [32]).

6 Room-temperature diffusive phenomena at interfaces of III–V semiconductors Room-temperature diffusion is not common in semiconductors. Typically diffusion is mediated by native defects such as vacancies and interstitials [33]. In Si, the formation energies of these defects are quite large, more than 3 eV, leading to very low concentrations. Thus, even though migration energies are very small, room-temperature diffusion is negligible. In doped III–V compound semiconductors, vacancy formation energies tend to be smaller [34], but migration energies go up because vacancies must hop to a second-neighbor site.

Recent data on GaN/AlGaN HEMTs found an unusual degradation mode by void formation at the interface between the AlGaN layer and the gate, at the corner on the drain side, at electric fields larger than a critical value, but without currents (Fig. 8) [35, 36]. Voiding has all the signs of diffusion as in electromigration, but the latter requires currents and occurs mostly in metals. The observed voiding was attributed to a critical value of strain that triggers diffusion, with the critical strain reached at a critical electric field (piezoelectric strain).

Calculations [37] found that something fairly unique happens in this case. With the Fermi level near the conduction band edge, the formation energy of triply-negatively charged vacancies is essentially zero (clearly an equilibrium concentration of vacancies is never achieved, otherwise the crystal would be unstable). Their migration energy, however, is quite large, ~1.6 eV (Fig. 8). The biaxial mismatch strain in the AlGaN has a minimal effect on the migration barrier and so does any additional strain coming

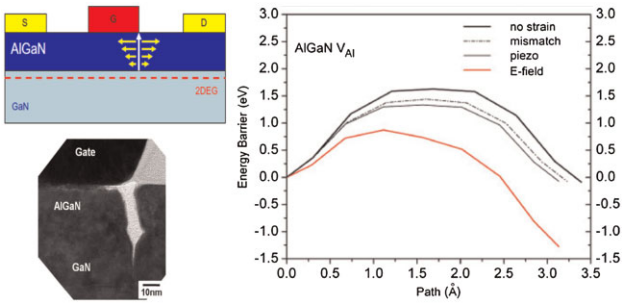

Figure 8 (online color at: www.pss-a.com) Left top: Schematic diagram of a HEMT. Left bottom: image of degradation by voiding (from Ref. [36]). Right: Calculated migration barrier for Al vacancies in AlGaN with no strain (perfect bulk), biaxial mismatch strain, strain caused by the electric field (piezo strain), and direct lowering of the barrier by the electric field. From Ref. [37].

from the piezoelectric effect at the critical field value. The electric field itself, however, tilts the barrier substantially because of the three negative charges (Fig. 8), leading to a net barrier of just under 1 eV, a signal that room-temperature diffusion becomes appreciable, offering an explanation for the observed voiding.

7 Concluding remarks This brief review has focused primarily on defects within extended defects such as grain boundaries and interfaces. Such defects can cause performance problems in devises. If they are successfully passivated, they can cause degradation under operating conditions or in harsh environments such as radiation by gradually being depassivated. A few examples were given to illustrate the power of combining theoretical calculations with experimental data to unravel the microscopic processes that cause degradation.

Acknowledgements The work described here was partially supported by the Air Force Office of Scientific Research and the Office of Naval Research through the MURI program, by the National Science Foundation, by the Department of Energy Basic Energy Sciences, by a DARPA/EPRI joint grant, and by the McMinn Endowment at Vanderbilt University. Contributions by R. Buczko, M. F. Chisholm, G. Y. Chung, S. Dhar, G. Duscher, L. C. Feldman, D. M. Fleetwood, A. Franceschetti, A. Maiti, K. McDonald, S. J. Pennycook, Y. S. Puzyrev, S. N. Rashkeev, T. Roy, R. D. Schrimpf, X. Shen, L. Tsetseris, S. Wang, K. H. Warnick, R. A. Weller, J. R. Williams, Y. Yan are gratefully acknowledged.

References

[1] A. Maiti, M. F. Chisholm, S. J. Pennycook, and S. T. Pantelides, Phys. Rev. Lett. **77**, 1306 (1996).
[2] M. Ramamoorthy and S. T. Pantelides, Phys. Rev. Lett. **76**, 4753 (1996).
[3] M. F. Chisholm, A. Maiti, S. J. Pennycook, and S. T. Pantelides, Phys. Rev. Lett. **81**, 132 (1998).
[4] Y. Yan, M. F. Chisholm, G. Duscher, A. Maiti, S. J. Pennycook, and S. T. Pantelides, Phys. Rev. Lett. **81**, 3675 (1998).
[5] L. Tsetseris and S. T. Pantelides, Phys. Rev. Lett. **97**, 116101 (2006).

[6] V. V. Afanasev, M. Bassler, G. Pensl, and M. Schulz, Phys. Status Solidi A **162**, 321 (1997).
[7] S. T. Pantelides, L. Tsetseris, S. N. Rashkeev, X. J. Zhou, D. M. Fleetwood, and R. D. Schrimpf, Microelectron. Reliab. **47**, 903 (2007).
[8] S. T. Pantelides, L. Tsetseris, M. J. Beck, S. N. Rashkeev, G. Hadjisavvas, I. G. Batyrev, B. R. Tuttle, A. G. Marinopoulos, X. J. Zhou, D. M. Fleetwood, and R. D. Schrimpf, Solid State Electron. **54**, 841 (2010).
[9] S. N. Rashkeev, D. M. Fleetwood, R. D. Schrimpf, and S. T. Pantelides, Phys. Rev. Lett. **87**, 165506 (2001).
[10] E. W. Enlow, R. L. Pease, W. E. Combs, R. D. Schrimpf, and R. N. Nowlin, IEEE Trans. Nucl. Sci. **38**, 1342 (1991).
[11] S. C. Witczak, R. D. Schrimpf, D. M. Fleetwood, K. F. Galloway, R. C. Lacoe, D. C. Mayer, J. M. Puhl, R. L. Pease, and J. S. Suehle, IEEE Trans. Nucl. Sci. **44**, (1989). (1997.
[12] S. N. Rashkeev, C. R. Cirba, D. M. Fleetwood, R. D. Schrimpf, S. C. Witczak, A. Michez, and S. T. Panelides, IEEE Trans. Nucl. Sci. **49**, 2650 (2002).
[13] S. C. Witczak, R. C. Lacoe, M. R. Shaneyfelt, D. C. Mayer, J. R. Schwank, and P. S. Winokur, IEEE Trans. Nucl. Sci. **47**, 2281 (2000).
[14] C. T. Sah, J. Y. C. Sun, and J. J. T. Tzou, Appl. Phys. Lett. **43**, 204 (1983).
[15] J. I. Pankove, D. E. Carlson, J. E. Berkeyheiser, and R. O. Wance, Phys. Rev. Lett. **51**, 2224 (1983).
[16] N. M. Johnson, C. Herring, and D. J. Chadi, Phys. Rev. Lett. **56**, 760 (1986).
[17] S. T. Pantelides, Appl. Phys. Lett. **60**, 995 (1987).
[18] P. J. H. Denteneer, C. G. Van de Walle, and S. T. Pantelides, Phys. Rev. B **39**, 10809 (1989).
[19] P. E. Blöchl, C. G. Van de Walle, and S. T. Pantelides, Phys. Rev. Lett. **64**, 1401 (1990).
[20] S. N. Rashkeev, D. M. Fleetwood, R. D. Schrimpf, and S. T. Pantelides, IEEE Trans. Nucl. Sci. **50**, 1896–1900 (2003).
[21] K. O. Jeppson and C. M. Svensson, J. Appl. Phys. **48**, (2004). (1977.
[22] D. K. Schroder and J. A. Babcock, J. Appl. Phys. **93**, 1 (2003).
[23] L. Tsetseris, X. J. Zhou, D. M. Fleetwood, R. D. Schrimpf, and S. T. Pantelides, Appl. Phys. Lett. **86**, 142103 (2005).
[24] G. Y. Chung, C. C. Tin, J. R. Williams, K. McDonald, M. Di Ventra, S. T. Pantelides, L. C. Feldman, and R. A. Weller, Appl. Phys. Lett. **76**, 1713 (2000).
[25] S. Wang, S. Dhar, S. Wang, A. C. Ahyi, A. Franceschetti, J. R. Williams, L. C. Feldman, and S. T. Pantelides, Phys. Rev. Lett. **98**, 026101 (2007).
[26] S. T. Pantelides, S. Wang, A. Franceschetti, R. Buczko, M. Di Ventra, S. N. Rashkeev, L. Tsetseris, M. H. Evans, I. G. Batyrev, L. C. Feldman, S. Dhar, K. McDonald, R. A. Weller, R. D. Schrimpf, D. M. Fleetwood, X. J. Zhou, J. R. Williams, C. C. Tin, G. Y. Chung, T. Isaacs-Smith, S. R. Wang, S. J. Pennycook, G. Duscher, K. van Benthem, and L. M. Porter, Mater. Sci. Forum **527**, 935 (2006).
[27] S. Wang, M. Di Ventra, S. G. Kim, and S. T. Pantelides, Phys. Rev. Lett. **86**, 5946 (2001).
[28] X. Shen and S. T. Pantelides, Appl. Phys. Lett. **98**, 053507 (2011).
[29] R. Buczko, S. J. Pennycook, and S. T. Pantelides, Phys. Rev. Lett. **84**, 943 (2000).
[30] M. Ramamoorthy and S. T. Pantelides, Phys. Rev. Lett. **76**, 267 (1996).
[31] M. Needels, J. D. Joannopoulos, Y. Bar-Yam, and S. T. Pantelides, Phys. Rev. B **43**, 4208 (1991).
[32] M. Di Ventra and S. T. Pantelides, J. Electron. Mater. **29**, 353 (2000).
[33] R. Car, P. J. Kelly, A. Oshiyama, and S. T. Pantelides, Phys. Rev. Lett. **52**, 1814 (1984); Phys. Rev. Lett. **54**, 360 (1985).
[34] C. G. Van de Walle and J. Neugebauer, J Appl. Phys. **95**, 3851 (2004).
[35] J. Joh and J. A. del Alamo, IEEE Electron Dev. Lett. **29**, 287 (2008).
[36] S. Y. Park, T. Lee, and M. J. Kim, IEEE Trans. Electron. Mater. **11**, 49 (2010).
[37] K. H. Warnick, Y. Puzyrev, T. Roy, D. M. Fleetwood, R. D. Schrimpf, and S. T. Pantelides, Phys. Rev. B **84**, 214109 (2011).

